



ELSEVIER

Available online at www.sciencedirect.com

SCIENCE @ DIRECT®

Physics Letters A 314 (2003) 44–50

PHYSICS LETTERS A

www.elsevier.com/locate/pla

Complicated basins in external-cavity semiconductor lasers

Awadhesh Prasad ^{a,*}, Ying-Cheng Lai ^{a,b}, Athanasios Gavrielides ^c, Vassilios Kovanis ^c

^a Department of Mathematics and SSERC, Arizona State University, Tempe, AZ 85287, USA

^b Departments of Electrical Engineering and Physics, Arizona State University, Tempe, AZ 85287, USA

^c Nonlinear Optics Center, Air Force Research Laboratory, DELO, Kirtland AFB, New Mexico, NM 87117, USA

Received 26 November 2002; received in revised form 24 March 2003; accepted 23 May 2003

Communicated by A.P. Fordy

Abstract

We demonstrate that complicated basins of attraction can occur in time-delay coupled, external-cavity semiconductor lasers. In particular, we find that there can be multiple coexisting attractors associated with low-frequency fluctuations in the laser power output, and prediction of the asymptotic attractor for specific initial conditions is practically impossible.

© 2003 Elsevier B.V. All rights reserved.

PACS: 05.45.-a; 42.65.Sf; 42.55.Px

Keywords: Nonlinear dynamics; Optical chaos; Semiconductor lasers

There has been a continuous interest in the basin structure in nonlinear dynamical systems since the pioneering works in the early eighties [1–5]. A reason for such an interest concerns the predictability of asymptotic attractors when initial conditions are chosen in the vicinity of basin boundaries. Smooth boundaries are simple sets whose dimensions are one less than that of the phase space. For these boundaries, an improvement in the precision to specify the initial conditions results in an equal amount of improvement in the predictability of the asymptotic attractor. Fractal basins are open (e.g., contain open areas in two dimensions) but their boundaries contain fractal, chaotic

invariant sets [1]. Typically, the dimension of a fractal basin boundary is a fraction less than the phase-space dimension. As a consequence, a more precise specification of the initial conditions often results in a much smaller improvement in the probability to predict the attractor correctly. Riddled basins contain no open sets (e.g., no open area in two dimensions) and have dimensions close to that of the phase space [6–11]. For riddled basins, a vast reduction in the uncertainty to specify the initial conditions results in hardly any improvement in ability to predict the final attractor. Because of this serious physical consequence, the phenomenon of riddling has received quite a lot of recent attention [6–12].

Complicated basin structures such as fractal and riddled basins are important because they can occur in physical systems [2–5,7,8]. The purpose of this Letter

* Corresponding author.

E-mail address: awadhesh@enpc589.eas.asu.edu (A. Prasad).

is to present evidence that riddled-like basins¹ can occur in a class of nonlinear optical systems of recent interest, external-cavity semiconductor lasers which are mathematically described by delay differential equations. Despite the infinite dimensionality of the phase space in such systems, we are able to demonstrate that low-dimensional attractors can coexist, and the boundaries separating their basins of attraction can exhibit riddled-like features. Physically, these attractors are often associated with low-frequency fluctuations (LFFs) in the power output of the laser. We believe our result is important because it is a phenomenon that has not been noticed previously in the study of LFFs in external-cavity semiconductor lasers. Our result is also mathematically interesting because it is a demonstration of complicated basins in infinite-dimensional dynamical systems.

A brief background on external-cavity semiconductor lasers and LFFs is as follows. There has been a large variety of applications of semiconductor lasers nowadays such as optical data recording and optical-fiber communication. In these applications optical feedbacks are inevitably present, such as back-scattered light from the end mirrors of the laser cavity. There are also applications in which optical feedbacks are deliberately introduced to improve the performances of the laser such as the enhancement of the single longitudinal mode operation, spectral line narrowing, improved frequency stability, wavelength tunability, etc. [13]. While low levels of optical feedbacks can be advantageous [13,14], the performances of semiconductor lasers are usually degraded when the feedback is at moderate or high levels. In particular, at high feedback levels, the laser can enter the so-called *coherence collapse* regime [15] where the optical linewidth increases drastically. At moderate feedback levels, when the pumping current is close to the solitary threshold, the laser intensity can exhibit sudden, down-to-zero dropouts at irregular times, followed by a slow and gradual recovery after each dropout (LFFs) [16]. LFFs pose a difficulty in applications where a sustained laser power is needed. Physi-

cally, when optical feedback is present, the laser effectively possesses an external cavity that injects the optical field back into the original laser cavity. From the viewpoint of dynamics, a semiconductor laser without feedback is a relaxation oscillator. However, due to the time delay in optical feedback, it is necessary to use time-delay differential equations to describe external-cavity semiconductor lasers, leading to infinite-dimensional phase spaces. There can be a rich variety of dynamical phenomena in these lasers [15, 17–19].

A single mode external-cavity semiconductor laser² is modeled by a set of delay-differential equations, known as the Lang–Kobayashi (LK) equations [22], which describe the time evolutions of the complex electrical field $E(t)$ of a single longitudinal mode and the carrier density $n(t)$ averaged spatially over the laser medium. The equations can be written in a standard normalized form [23], as follows:

$$\begin{aligned} \frac{dE(t)}{dt} &= (1 + i\alpha)N(t)E(t) + \eta e^{-i\omega_0\tau} E(t - \tau), \\ T \frac{dN(t)}{dt} &= J - N(t) - [2N(t) + 1]|E(t)|^2, \end{aligned} \quad (1)$$

where α is the linewidth enhancement factor, ω_0 is the angular frequency of the solitary laser, τ_p is the photon life time, τ_s is the carrier lifetime, $J \equiv \mathcal{J} - \mathcal{J}_{\text{th}}$ (\mathcal{J} is the injected constant current density and \mathcal{J}_{th} is the threshold), $N(t) \equiv n(t) - n_{\text{th}}$, and $n_{\text{th}} = \tau_p^{-1}$ is the threshold carrier density for the solitary laser. The coefficient γ characterizes the relative amount of light reflected back into the laser cavity, while the delay time $\tau = 2L/c$ is the round-trip time of the light in the external cavity of length L . The two remaining parameters in the LK-equations are $\eta = \tau_p\gamma$ and $T = \tau_s/\tau_p$. The power of the laser is $P(t) = |E(t)|^2$ and the phase of the laser field is denoted by $\phi(t)$. The phase delay, $Z(t)$, is defined as $\phi(t) - \phi(t - \tau)$.

To demonstrate complicated basins, we consider a pair of time-delay coupled, external-cavity semiconductor lasers, as schematically illustrated in Fig. 1. The coupling between lasers L_1 and L_2 is characterized by the parameter $\eta_1 < 1$, i.e., a η_1 fraction of the

¹ To establish riddling mathematically is not feasible for realistic physical systems such as the external-cavity semiconductor lasers that we deal with in this Letter. Here we say a basin is riddled-like, based on numerical observation only.

² While LFFs can occur in multi-mode external-cavity semiconductor lasers (e.g., see Ref. [20]), there is also streak-camera evidence that single-mode lasers can exhibit LFFs (see, for example, Ref. [21] and references therein).

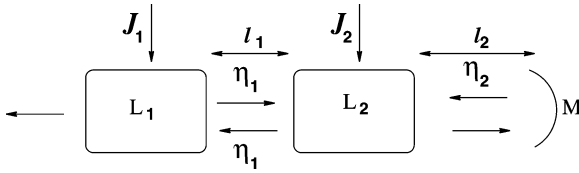


Fig. 1. Schematic illustration of a pair of time-delay coupled, external-cavity semiconductor lasers.

laser field of L_1 is injected into L_2 and vice versa. The reflection coefficient from mirror M , which forms the external cavity with laser L_2 , is η_2 . The physical distance between L_1 and L_2 is l_1 and the length of the external cavity of L_2 is l_2 . In this configuration, laser L_1 has an active feedback from laser L_2 while laser L_2 has two external feedbacks (one is active from laser L_1 and another is passive from mirror M). The coupled LK equations [24] are

$$\begin{aligned} \frac{dE_1(t)}{dt} &= (1 + i\alpha)N_1E_1(t) + \eta_1e^{-i\omega_1\tau_1}E_2(t - \tau_1), \\ T\frac{dN_1(t)}{dt} &= J_1 - N_1(t) - [2N_1(t) + 1]|E_1(t)|^2, \\ \frac{dE_2(t)}{dt} &= (1 + i\alpha)N_2E_2(t) + \eta_1e^{-i\omega_1\tau_1}E_1(t - \tau_1) \\ &\quad + \eta_2e^{-i\omega_2\tau_2}E_2(t - \tau_2), \\ T\frac{dN_2(t)}{dt} &= J_2 - N_2(t) - [2N_2(t) + 1]|E_2(t)|^2, \end{aligned} \quad (2)$$

where subscripts 1 and 2 are referred to lasers L_1 and L_2 , respectively, $\tau_1 = l_1/c$ and $\tau_2 = 2l_2/c$.

Fig. 2(a) shows the time evolution of power P for a single external-cavity laser for $T = 1000$, $\alpha = 6$, $\tau = 1000$, $J = 4 \times 10^{-3}$, $\eta = 2 \times 10^{-3}$ and $\omega\tau = -1$. The plot is apparently irregular and power can drop to nearly zero. In these calculations, other parameters values are $\omega_1 = -1/\tau$, $J_1 = 4 \times 10^{-3}$, $J_2 = 2 \times 10^{-3}$, $\eta_1 = 2 \times 10^{-3}$, $\tau_1 = \tau_2 = 1000$, and $\eta_2 = 3.3 \times 10^{-3}$. The bifurcation parameter is ω_2 . We utilize the fourth-order Adams–Bashford–Moulton (ABM) predictor–corrector method [25] with step size $dt = \tau_1/n_p$ to integrate Eq. (2), where $n_p = 1000$ is chosen to be the number of initial conditions in the time intervals $-\tau_{1,2} \leq t < 0$. At this sufficiently large n_p the numerical integration for this system, Eq. (2), is stable. For the coupled system, the output power $P_1(t)$ is more regular and its minimum values are bounded away from zero as shown in Fig. 2(b) for $\omega_2 = -1.5 \times 10^{-3}$. Here the amplitude of the power fluctuations

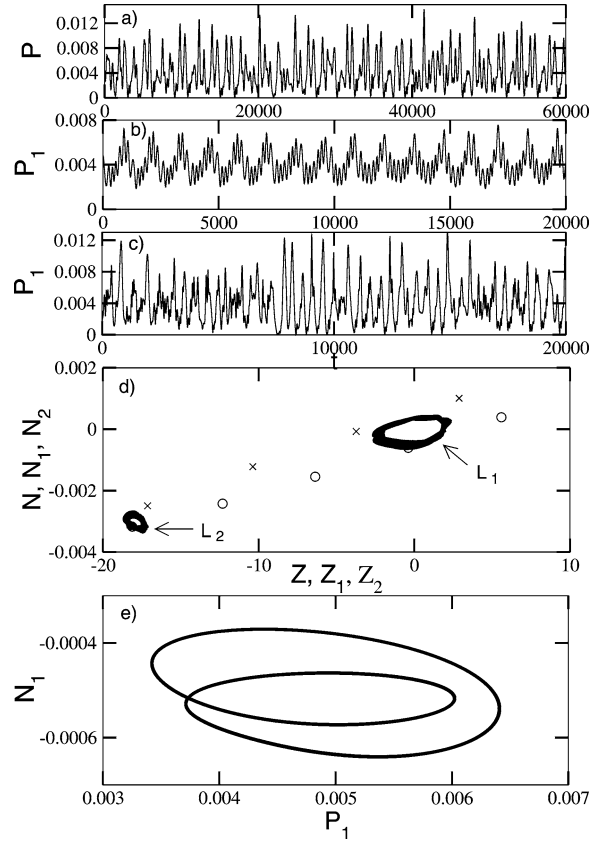


Fig. 2. Time traces of the power output: (a) uncoupled laser; and coupled system (Eq. (2)) at (b) $\omega_2 = -1.5 \times 10^{-3}$ and (c) $\omega_2 = -2 \times 10^{-4}$. (d) The trajectories of L_1 and L_2 in planes Z_1-N_1 and Z_2-N_2 , respectively, of coupled systems at $\omega_2 = -1.5 \times 10^{-3}$. The fixed points in $Z-N$ plane are those of the uncoupled laser L_2 . (e) The Poincaré section of the trajectory in (d) at $Z_1 = 0$, indicating its quasiperiodic nature.

is reduced but its average power output remains approximately the same as that of the uncoupled laser. This means that, the average output of the coupled laser system can be controlled by adjusting the amount of the injecting current J_1 . Thus, the coupled laser system can operate without degrading in power output but with the desirable feature that the instantaneous power will never be zero.

The absence of down-to-zero power drop in the coupled laser system can be explained by a stability analysis of the fundamental solutions of individual external-cavity semiconductor lasers, which constitute the dynamical invariant sets responsible for LFFs [21, 26]. The solutions are determined by the following set

of transcendental equations:

$$\begin{aligned}
 N_s &= -\eta \cos(\phi_0 + Z_s), & N_s &= \frac{J - P_s}{(1 + 2P_s)}, \\
 Z_s &= -\eta\tau \sqrt{1 + \alpha^2} \sin[Z_s + \phi_0 + \tan^{-1} \alpha], \\
 \eta^2 &= N_s^2 + (Z_s/\tau - \alpha N_s)^2,
 \end{aligned} \tag{3}$$

where the phase-delay variable is $Z(t) \equiv \phi(t) - \phi(t - \tau)$ and $Z_s = (\omega_s - \omega_0)\tau$. For a given set of parameters values, three different types of fixed points exist: a maximum-gain mode (MGM), a number of external-cavity modes (ECMs, circles) and antimodes (crosses). These are distributed along an elliptic curve in the (Z, N) plane, as shown in Fig. 2(d) at $\eta = 3.3 \times 10^{-3}$. A trajectory can never stay near any ECM or antimode for long time, giving rise to phenomenon such as LFFs [26,27]. When two lasers are coupled with a time delay, the ranges in the (Z, N) plane of these attractors are reduced dramatically, as shown in Fig. 2(d), where the upper-right attractor is that of laser L_1 and the lower-left attractor is from L_2 . We observe that both lasers operate more locally in the phase space: laser L_2 tends to stay near the MGM, while the dynamical trajectories of L_1 are confined in a phase-space region where the corresponding power can never be zero.

The features, as shown in Fig. 2(b) and (d), in fact occur in finite parameter regions, as shown in Fig. 3, where the maximum and minimum values of the power output of the coupled laser system are plotted versus the bifurcation parameter ω_2 . We see that there are *locked* parameter regions of finite size in which the minimum value of the power output is not zero. There are also *unlocked* regions for which the power can be zero; an example of the power time series is shown in Fig. 2(c) for $\omega_2 = -2 \times 10^{-3}$. Examination using Poincaré surface of sections for Fig. 2(b) and (c) indicate that former is quasiperiodic (Fig. 2(e) for laser L_1) while later is chaotic. We note that previous studies indicate that LFFs in external-cavity semiconductor lasers are the result of various chaotic transitions [21,26]. The dynamics of such lasers in the LFF regime are thus typically chaotic. As we see here, time-delayed coupling can convert the chaotic oscillation of the laser field with power dropouts into quasiperiodic motion without power dropouts.

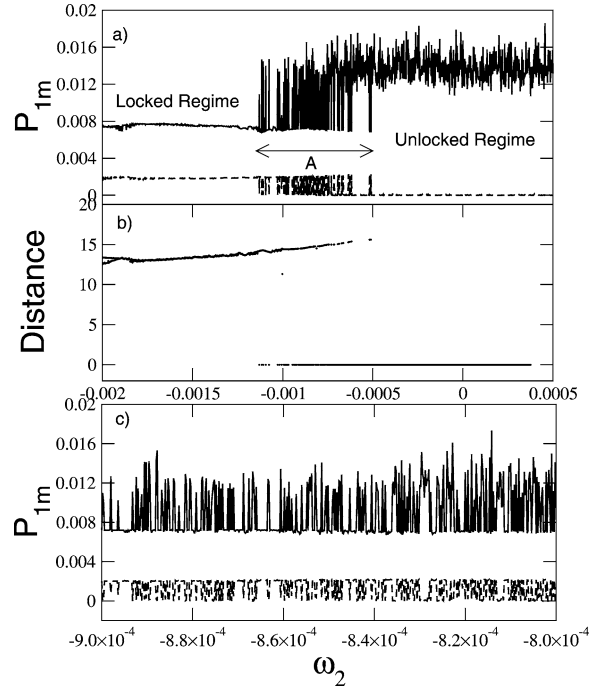


Fig. 3. (a) For the coupled laser system, the maximum (solid line) and minimum (dotted line) values of the power output versus ω_2 . (b) The minimum distance (dots) between the local attractors of lasers L_1 and L_2 versus ω_2 . (c) A blowup of part of the region A in (a).

A remarkable feature of Fig. 3 is that there appears to be a parameter interval in which the power output P_1 of the system exhibits wild fluctuations as a function of the bifurcation parameter, which is denoted by region A in Fig. 3(a). These fluctuations persist on small scales, as shown in a blowup of part A in Fig. 3(c). Such fluctuations typically indicate co-existing attractors with complicated basins [9,12]³ because a small change in the parameter can lead to a completely different attractor with distinct power-output characteristics. We find that one attractor is chaotic with down-to-zero drops in laser power and another is quasiperiodic without such power drops. The minimum distance between the local attractors of laser L_1 and L_2 , as shown in Fig. 3(b), also manifests this transition clearly. In the locked regime they are far apart (Fig. 2(d)) while in the unlocked region they overlapped on each other (making the distance zero).

³ It seems that the present bifurcation is “blurred blow-out” type of bifurcation as shown by Ashwin et al. in Ref. [12].

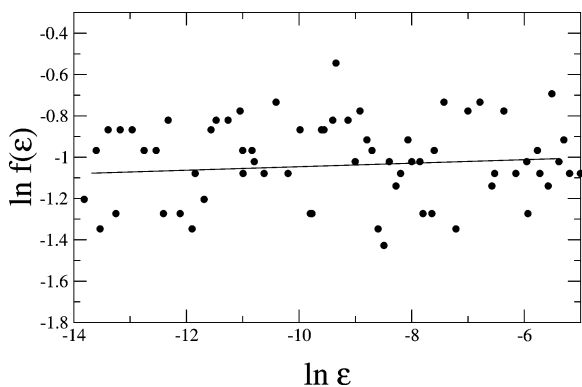


Fig. 4. Fraction $f(\epsilon)$ of uncertain parameter pairs (out of 100 parameter pairs) versus parameter perturbation ϵ for the parameter, ω_2 , interval marked as region A in Fig. 3(a).

However, in the region A, the presence of both the zero and the non-zero distances confirm the both type of scenarios. The sensitivity of the laser output on parameter variations can be conveniently quantified by the uncertainty exponent [1,4,9], as follows. We fix a small perturbation ϵ and randomly choose a pair of parameters of ϵ -distance apart in region A of Fig. 3(a). The two parameters are *uncertain* with respect to perturbation ϵ if they yield different attractors. The fraction of uncertain parameter pairs $f(\epsilon)$ typically decreases with ϵ and scales with ϵ as

$$f(\epsilon) \sim \epsilon^\beta, \quad (4)$$

where $\beta > 0$ is the uncertainty exponent [1,4,9]. Fig. 4 shows a typical plot of $f(\epsilon)$ versus ϵ , where we see that there are large fluctuations in $f(\epsilon)$. The feature to notice is, however, that as ϵ is reduced, $f(\epsilon)$ does not appear to decrease appreciably. In fact, a least-squares fit of the plot gives $\beta = 0.003 \pm 0.01$, indicating that β cannot be distinguished from zero. This is typical of riddled or riddled-like basins [9]. The practical implication is that the asymptotic attractor cannot be predicted, if there is an uncertainty in the specification of parameters and initial conditions, no matter how small. Indeed, the basins of the chaotic and quasiperiodic attractor appear to be interwoven with apparent lack of structures, as shown in Fig. 5(a) and (b) for $\omega_2 = -8 \times 10^{-4}$, where the dots denote initial conditions that go to the chaotic attractor and (b) is a

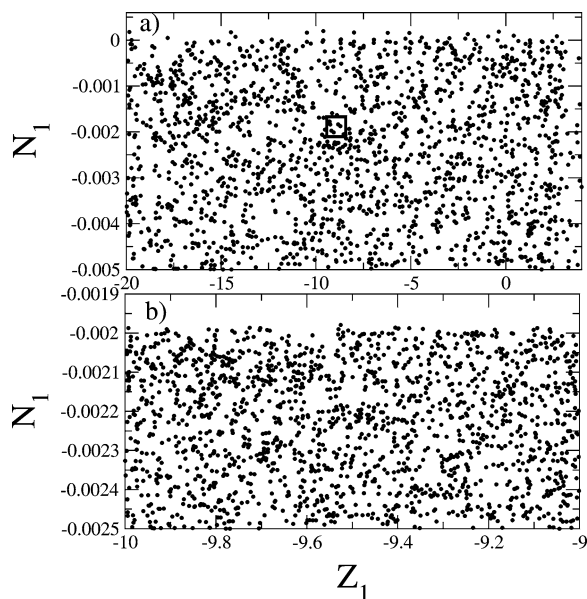


Fig. 5. The basin of the chaotic attractor (black dots) for $\omega_2 = -8 \times 10^{-4}$. (b) A blowup of part of (a).

blowup of part of (a).⁴ We find that no matter how small the phase-space region is chosen to be, there are always two classes of initial conditions mixed in a riddled-like manner which go to the two different attractors. Figs. 4 and 5 are thus a clear demonstration of the phenomenon of riddled-like basins in external-cavity semiconductor lasers.

In summary, we have presented numerical evidence for the occurrence of riddled-like basins in a realistic nonlinear optical system: coupled external-cavity semiconductor lasers. To our knowledge, prior to this Letter the issues of multiple coexisting attractors and the associated basin topologies have been largely ignored in the study of such lasers. A practical implication is that in the actual operation, the presence of small perturbations in parameters or in laser fields can cause the laser to move between the coexisting attractors and the power output can change wildly.

⁴ The technical details for generating Fig. 5 are as follows. We start with a randomly selected initial condition in the plane (Z_1, N_1) , keeping remaining variables $(6 \times 10^3 - 2)$ fixed. After removing sufficient transients, 6×10^5 , we check whether the motion (within next 1×10^5 data points) is quasiperiodic or chaotic. This is quantified by the value of P_{\max} (Fig. 3) whether it is below a threshold, $P_{\max} = 0.009$, or above it for the respective attractors.

The riddled-like basin structure suggests that such changes cannot be predicted or controlled even in principle.

We stress that, while complex basins have indeed been studied extensively, the existence of such basins in a realistic physical system described by complex delay-differential equations has not been observed prior to our work. Our work represents a good example where interesting phenomena in nonlinear dynamics, usually studied using relatively simple mathematical models, can in fact occur in physical systems. More importantly, as we have shown in our work, concepts in nonlinear dynamics can be useful for understanding realistic physical devices. For instance, in lasers, the presence of small perturbations in parameters or in fields can cause the laser to move between the co-existing attractors, resulting in wild fluctuations in the power output. One may try to reduce the environmental noise to suppress the fluctuations, but our work shows that this is practically impossible because of the intrinsic dynamical property of riddling.

Acknowledgement

This work is supported by AFOSR under Grant No. F49620-98-1-0400.

References

- [1] C. Grebogi, S.W. McDonald, E. Ott, J.A. Yorke, *Phys. Lett. A* 99 (1983) 415;
C. Grebogi, E. Ott, J.A. Yorke, *Phys. Rev. Lett.* 50 (1983) 935.
- [2] F.T. Arecchi, R. Badii, A. Politi, *Phys. Rev. A* 29 (1984) 1006;
F.T. Arecchi, A. Califano, *Phys. Lett. A* 101 (1986) 443.
- [3] F.C. Moon, *Phys. Rev. Lett.* 53 (1984) 962;
F.C. Moon, G.-X. Li, *Phys. Rev. Lett.* 55 (1985) 1439.
- [4] S.W. McDonald, C. Grebogi, E. Ott, J.A. Yorke, *Physica D* 17 (1985) 125;
C. Grebogi, E. Kostelich, E. Ott, J.A. Yorke, *Physica D* 25 (1987) 347.
- [5] E.G. Gwinn, R.M. Westervelt, *Phys. Rev. A* 33 (1986) 4143.
- [6] J.C. Alexander, J.A. Yorke, Z. You, I. Kan, *Int. J. Bifurc. Chaos* 2 (1992) 795.
- [7] E. Ott, J.C. Alexander, I. Kan, J.C. Sommerer, J.A. Yorke, *Physica D* 76 (1994) 384.
- [8] J.F. Heagy, T.L. Carroll, L.M. Pecora, *Phys. Rev. Lett.* 73 (1994) 3528.
- [9] Y.-C. Lai, R.L. Winslow, *Phys. Rev. Lett.* 72 (1994) 1640.
- [10] Y.-C. Lai, C. Grebogi, *Phys. Rev. E* 52 (1995) R3313;
- Y.-C. Lai, C. Grebogi, J.A. Yorke, S.C. Venkataramani, *Phys. Rev. Lett.* 77 (1996) 55;
- Y.-C. Lai, C. Grebogi, *Phys. Rev. Lett.* 77 (1996) 5047;
- Y.-C. Lai, *Phys. Rev. E* 56 (1997) 3897;
- Y.-C. Lai, C. Grebogi, *Phys. Rev. Lett.* 83 (1999) 2926.
- [11] P. Ashwin, J. Buescu, I.N. Stewart, *Phys. Lett. A* 193 (1994) 126;
P. Ashwin, J. Buescu, I.N. Stewart, *Nonlinearity* 9 (1996) 703;
H. Nakajima, Y. Ueda, *Physica D* 99 (1996) 35;
L. Billings, J.H. Curry, E. Phipps, *Phys. Rev. Lett.* 79 (1997) 1018;
K. Kaneko, *Phys. Rev. Lett.* 78 (1997) 2736;
Y.L. Maistrenko, V.L. Maistrenko, A. Popovich, E. Mosekilde, *Phys. Rev. E* 57 (1998) 2713;
T. Kapitaniak, Y. Maistrenko, A. Stefanski, J. Brindley, *Phys. Rev. E* 57 (1998) R6253;
M. Woltering, M. Markus, *Phys. Rev. Lett.* 84 (2000) 630.
- [12] P. Ashwin, E. Covas, R. Tavakol, *Nonlinearity* 12 (1999) 563.
- [13] K.R. Preston, K.C. Woolard, K.H. Kameron, *Electron. Lett.* 17 (1981) 931;
K. Kikuchi, T. Okoshi, *Electron. Lett.* 18 (1982) 10;
L. Goldberg, H.F. Tylor, A.A. Dandridge, J.F. Weller, R.O. Miles, *IEEE J. Quantum Electron.* 18 (1982) 555;
S. Saito, O. Nilsson, Y. Yamamoto, *IEEE J. Quantum Electron.* 18 (1982) 961;
R. Wyatt, W.J. Devlin, *Electron. Lett.* 19 (1983) 110;
F. Favre, D. Le Guen, *Electron. Lett.* 19 (1983) 663.
- [14] R.W. Tkach, A.R. Chraplyvy, *J. Lightwave Technol.* 4 (1986) 1655.
- [15] D. Lenstra, B.H. Verbeek, A.J. den Boef, *IEEE J. Quantum Electron.* 21 (1985) 674.
- [16] C. Risch, C. Voumard, *J. Appl. Phys.* 48 (1977) 2083.
- [17] J. Sacher, W. Elsässer, E.O. Göbel, *Phys. Rev. Lett.* 63 (1988) 2224;
J. Sacher, W. Elsässer, E.O. Göbel, *IEEE J. Quantum Electron.* 27 (1991) 373;
J. Mørk, B. Tromborg, P.L. Christiansen, *IEEE J. Quantum Electron.* 24 (1988) 123;
B. Tromborg, J. Mørk, *IEEE J. Quantum Electron.* 26 (1990) 642;
H. Olesen, J.H. Osmundsen, B. Tromborg, *IEEE J. Quantum Electron.* 22 (1986) 762;
S. L. Woodward, T.L. Koch, U. Koren, *IEEE Phot. Technol. Lett.* 2 (1990) 391.
- [18] G.C. Dente, P.S. Durkin, K.A. Wilson, C.E. Moeller, *IEEE J. Quantum Electron.* 24 (1988) 2441.
- [19] S. Wiczorek, B. Krauskopf, D. Lenstra, *Opt. Commun.* 172 (1999) 279;
B. Krauskopf, D. Lenstra (Eds.), *Fundamental Issues of Nonlinear Laser Dynamics*, AIP Conference Proceedings, Vol. 548, AIP, Melville, NY, 2000.
- [20] G. Vaschenko, M. Giudici, J.J. Rocca, C.S. Menoni, J.R. Tredicce, S. Balle, *Phys. Rev. Lett.* 81 (1998) 5536.
- [21] R.L. Davidchack, Y.-C. Lai, A. Gavrielides, V. Kovanis, *Physica D* 145 (2000) 130;
R.L. Davidchack, Y.-C. Lai, A. Gavrielides, V. Kovanis, *Phys. Rev. E* 63 (2001) 056206.

- [22] R. Lang, K. Kobayashi, *IEEE J. Quantum Electron.* 16 (1980) 347.
- [23] P.M. Alsing, V. Kovanis, A. Gavrielides, T. Erneux, *Phys. Rev. A* 53 (1996) 4429.
- [24] A. Prasad, Y.-C. Lai, A. Gavrielides, V. Kovanis, Preprint, 2003.
- [25] W.H. Beyer (Ed.), *CRC Standard Mathematical Tables and Formulae*, 29th Edition, CRC Press, Boca Raton, FL, 1991.
- [26] T. Sano, *Phys. Rev. A* 50 (1994) 2719.
- [27] A. Prasad, Y.-C. Lai, A. Gavrielides, V. Kovanis, *J. Opt. B: Quantum Semiclass. Opt.* 3 (2001) 242.